AD-A058 677 NAVAL ACADEMY ANNAPOLIS MD F/G 20/2
RADIATION INDUCED DIELECTRIC RELAXATION IN RARE-EARTH DOPED CAL--ETC(U)
MAY 78 G C KOLODZIEJCZAK
UNCLASSIFIED USNA-TSPR-93 NL

1 OF 1
AD
A058 677

END
DATE
FILMED
-11-78
DDC

LEVEL II

A TRIDENT SCHOLAR PROJECT REPORT

NO. 93

"RADIATION INDUCED DIELECTRIC RELAXATION IN RARE-EARTH DOPED CALCIUM FLUORIDE"

UNITED STATES NAVAL ACADEMY
ANNAPOLIS, MARYLAND
1978

"Radiation Induced Dielectric Relaxation in Rare-Earth Doped Calcium Fluoride"

A Trident Scholar Project Report

by

Midshipman Greg C. Kolodziejczak, Class of 1978

U. S. Naval Academy

Annapolis, Maryland

Richard L. Johnston

Assoc. Prof. Richard L. Johnston
Physics Department

John Fontanella

Advisor: Asst. Prof. John Fontanella
Physics Department

Accepted for Trident Scholar Committee

Chairman

25 MAY 1978

Date

ABSTRACT

Low frequency dielectric properties of rare-earth doped calcium fluoride crystals were studied over a temperature range of 5.5°K to 380°K. Low flux neutron radiation was found to have no effect. Gamma-rays, on the other hand, were found to significantly affect these properties. Although the specific effects depended heavily on the dopant and its concentration, generally R_1 and R_2 increase, R_3 and R_4 decrease, and a new peak between R_2 and R_3 is created. The crystals had not yet reached a state of dielectric equilibrium when removed from the gamma-ray source; therefore, time studies were conducted which revealed that changes in existing peaks were stable, whereas the new peaks gradually decayed back to zero. Studies were also done on how the effects varied with dose. Variations were found, but most of the effects occurred at the lowest dose studied. The results support the hypothesis that R_1 is from isolated dipoles, R_2 is from simple clusters, and R_3, R_4 and R_5 are from more complex clusters. The possible use of dielectrics in dosimetry is discussed.

ACKNOWLEDGEMENTS

Any endeavor into the scientific realm is really a group effort, so the author would like to thank all those who supported the efforts behind this project. Most importantly, thanks go to Drs. John Fontanella and Richard Johnston for their continuous help and knowledge in advising this project.

Special thanks are also extended to Dr. Carl Andeen of Case Western Reserve University for the excellent equipment used in the study.

Finally, the author is deeply indebted to Miss Debbie Kelly, Sharon Mark, and Debbie Queen for their patience and typing expertise in the final preparation of this paper.

Greg C. Kolodziejczak
17 May 1978
Annapolis, Maryland

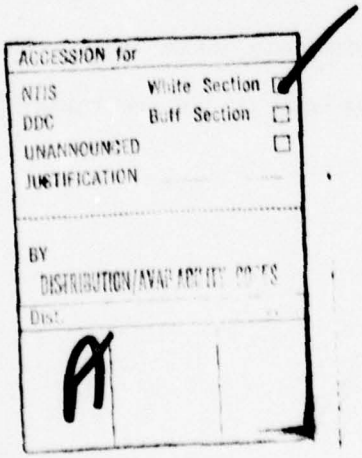

TABLE OF CONTENTS

I. INTRODUCTION

A dielectric, by definition, is an insulator. The dielectric studied here, calcium fluoride (CaF_2), is a crystal which may be thought of as a simple cubic array of fluorines with a calcium occupying every other cube, as shown in Figure 1. When the crystal has been doped, rare-earth ions replace some of the calcium ions in the

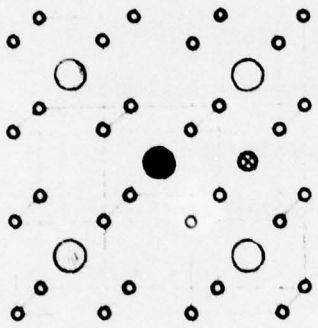

Figure 1. Crystal structure of calcium fluoride with a dipole caused by rare-earth doping. The white circles are fluorines; gray are calciums; the black circle is a rare-earth; and the one marked with an X is an interstitial fluorine.

crystal lattice. Since rare-earths are trivalent (3^+) and calcium is divalent (2^+), this creates a charge imbalance. One mechanism for compensating this imbalance is the addition of more fluorine ions to the material. Such an ion, which is not part of the lattice structure itself and is probably located in an empty cube, is called interstitial. If located in the cube adjacent to the rare-earth ion, it is called a

local (or nearest neighbor) charge compensator. Thus, in this situation there is a quasi - permanent dipole consisting of the rare-earth ion and the interstitial fluorine. Considerable research in the past few years, however, has proven that this simplistic model is inadequate to describe the behavior of the dielectric over a wide temperature range. In fact, it has been shown that at least five other charge configurations (or multiple ion motions resulting from the same charge configuration) exist in the material.[1-4] The current work increases the complexity further by reporting still another type of charge configuration, this one being radiation induced. The theory underlying this study will, therefore, be presented using the simple dipole model, then later expanded to incorporate other possible charge configurations.

II. BASIC DIELECTRIC THEORY

A. The Dielectric Constants

The complex dielectric constant consists of a real and imaginary part, the former (ε') being a measure of capacitance and the latter (ε'') being proportional to conductance. Both are related to the polarization of bound charges in a nonconductor that is subjected to an electric field. Capacitance deals with the ability of the charges to polarize, and conductance is a measure of the energy dissipation from the polarization. First consider a capacitor with a vacuum between its plates, as shown in Figure 2a.

Figure 2. (a) Capacitor in vacuum; (b) Capacitor filled with a dielectric. (From V. V. Daniel in Dielectric Relaxation, New York: Academic Press, Inc., 1967, p. 14.)

The capacitance of this system is denoted by C_o. Since capacitance is defined as

$$C = \frac{Q}{V} \tag{1}$$

where Q is the plate charge and V is the potential difference between the plates, it is simple to calculate

the capacitance of the system in Figure 2a to be

$$C_o = \frac{\varepsilon_o A}{d} \tag{2}$$

where ε_o is the permittivity of the free space, A is the plate area, and d is the distance between the plates. Now suppose a dielectric material is introduced between the plates and completely fills the space there, as in Figure 2b. When the electric field is applied, the negative charges in the material move slightly toward the positive plate and the positive charges move slightly toward the negative plate. When the material contains permanent dipoles, such as those discussed in doped calcium fluoride, these dipoles also align with the field. This polarization, or charge displacement, compensates part of the plate charge so that the electric field through the material is reduced. For a fixed charge, the potential difference between the plates is therefore reduced, and, from equation (1), the capacitance increases. The real dielectric constant of the material is defined as the ratio of the capacitance with the material present to the vacuum capacitance.

$$\varepsilon' = \frac{C}{C_o} \tag{3}$$

Next consider the subject of energy dissipation.

In a conductor such as metal, the application of an electric field causes free electrons to move through the material, thus creating a current. Energy is dissipated by a current i flowing through a material of electrical resistance R at the rate

$$P = i^2 R \tag{4}$$

This is, of course, called power, and the units are energy per unit time. In a dielectric, there are no free electrons to create a current. However, the existence of permanent dipoles supplies what the author will term locally free ions, in that the negative ions (interstitial fluorines) are somewhat free to move around the positive ions (rare-earths). Just as the motion of electrons through a conductor causes an energy loss, so does the motion of the ions in a dielectric. This loss is characterized by a parameter called dielectric conductivity and denoted by σ''. It has units of energy per unit time and is a function of the number of ions moving and the resistance to them moving. Suppose the material in Figure 2b is a rare-earth doped calcium fluoride, which has a permanent dipole. In this situation, the dipoles would align themselves with the field, and there would be no further motion. Consequently, there is no steady

state energy dissipation. However, suppose the field through the dielectric alternated with frequency. Then the dipoles would be continually aligning themselves with the field; there would be continual energy dissipation; and σ'' would have a finite value. The imaginary dielectric constant is related to σ'' by

$$\varepsilon'' = \frac{\sigma''}{\varepsilon_o \omega} \tag{5}$$

As can be seen from this, ε'' is a measure of the energy dissipation per cycle of the alternating field rather than per unit time.

B. Relaxation Time

Relaxation, in general terms, is the process in which there is a delayed response to a stimulus. Specifically, the delay is an exponential function of certain system parameters. For example, dipoles in a dielectric do not align instantly with an electric field. Therefore, dipole alignment is a delayed response to a stimulus, the electric field. As such, it is characterized by a relaxation time, τ. This relaxation time can be mathematically formulated by considering the bistable model of local charge transport, shown in Figure 3.

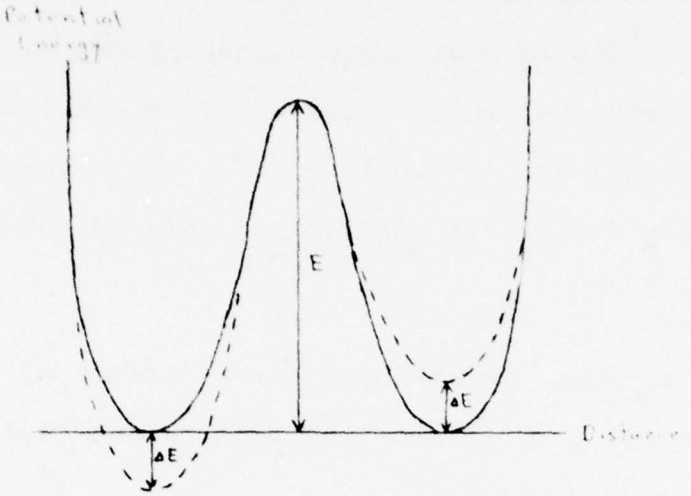

Figure 3. The bistable model. The potential energy as a function of distance has two minima, "potential wells," whose depth is modified by an applied electric field. The two wells contain one ion which may occupy either well. (From V. V. Daniel, op. cit., p. 21.)

The plot shows potential energy as a function of position. The ion (for the purposes of this study, the interstitial fluorine) may occupy either of two sites of minimum potential energy. In relation to a calcium fluoride crystal, these two sites are the empty cubes on either side of a rare-earth ion. The ions must overcome a potential barrier of height E (called the activation energy) in order to get from one site to the other. When an electric field acts on the system, the wells are distorted, as indicated by the dotted line. Each ion in its well oscillates with a characteristic frequency f_o. Generally it

cannot make the jump to the other site because it lacks sufficient energy. However, from statistical thermodynamics, it occasionally acquires the energy and makes the jump with frequency

$$f = f_o e^{-E/kT} \tag{6}$$

where k is Boltzmann's constant (8.6205×10^{-5} eV/K) and T is absolute temperature in degrees Kelvin. The jumps are, of course, random and have no net effect unless an electric field is applied, in which case jumps into one site are favored over jumps into the other.

$$f = f_o e^{-(E \pm \Delta E)/kT} \tag{7}$$

where ΔE is the change in the potential well caused by the applied field. It is clear that the higher the frequency of jumps is, the quicker the dipoles will be able to align, and the shorter the relaxation time will be. In fact, relaxation time is given by the reciprocal of equation (6):

$$\tau = \tau_o e^{E/kT}$$

The precise quantitative meaning of τ is shown in Figure 4.

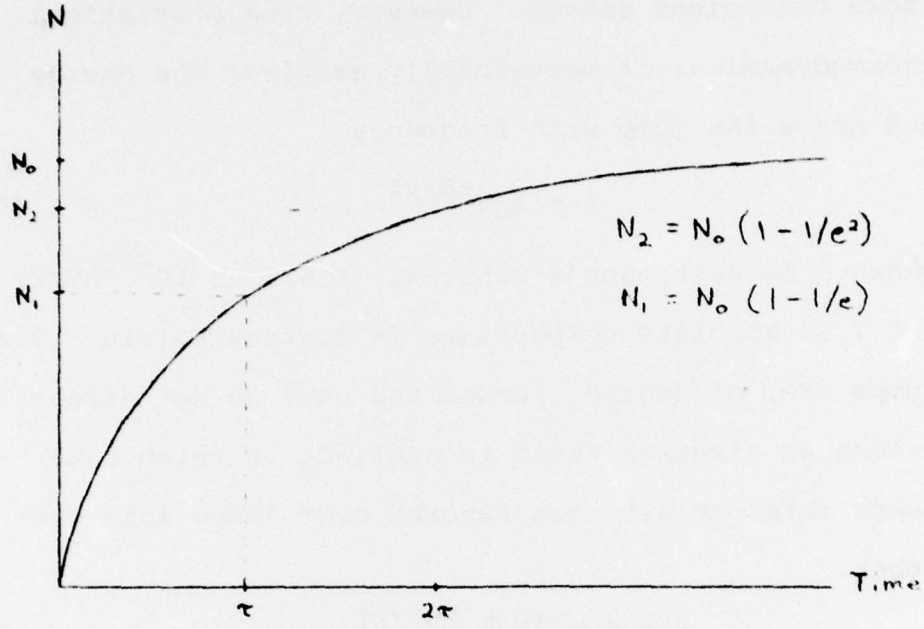

Figure 4. Dipole alignment as a function of time. The diagram represents a total of N_O dipoles which were subjected to an electric field at time t = o. the number of them that have aligned is plotted as a function of time. The number that have not yet aligned decreases by a factor of e after each period of the relaxation time. Thus, τ is a measure of the response time of the dipoles.

C. Frequency Dependence

Given the concept of relaxation time, it is easy to understand how the dielectric constants should

vary with frequency. First consider polarization as a function of frequency. In addition to the dipolar polarization which has already been discussed, there is also ionic and electronic polarization. Ionic polarization is the displacement of the ions in the crystal lattice structure itself. In calcium fluoride, the calcium ions would displace slightly to the negative electrode and the fluorine ions to the positive electrode. Electronic polarization arises from the electrons orbiting the nucleus. Again there is a slight displacement, this time between the nucleus and the orbital shell. Because of the speed with which electrons orbit the nucleus, this can occur at frequencies up to the ultraviolet region. Ionic polarization extends to the infrared region, and dipolar polarization extends through UHF to microwaves. Thus, the relaxation time is the longest for the dipoles and the shortest for the electrons in their respective motions. A plot of this is shown in Figure 5.

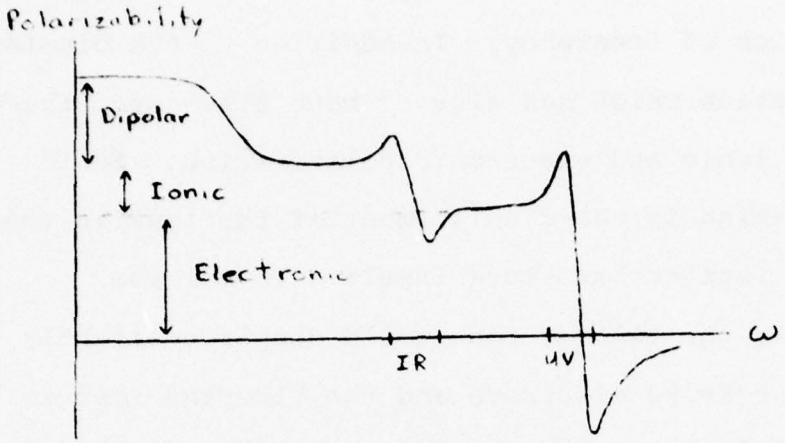

Figure 5. Frequency dependence of the various forms of polarization. (From Introduction to Solid State Physics, edited by C. Kittel. New York: John Wiley and Sons Inc., 1971, p. 461)

The peaks are from resonances. An interesting note here is that the real dielectric constant (ε') between the infrared and ultraviolet regions (in the optical range) is equal to the square of the refractive index, by definition.

$$\varepsilon'_{(IR-UV)} = n^2 \qquad (9)$$

In the present study, however, it is sufficient to concern ourselves only with the dipolar region. This region is redrawn and labeled in Figure 6. Here it is plotted against log ($\omega\tau$), a unitless parameter,

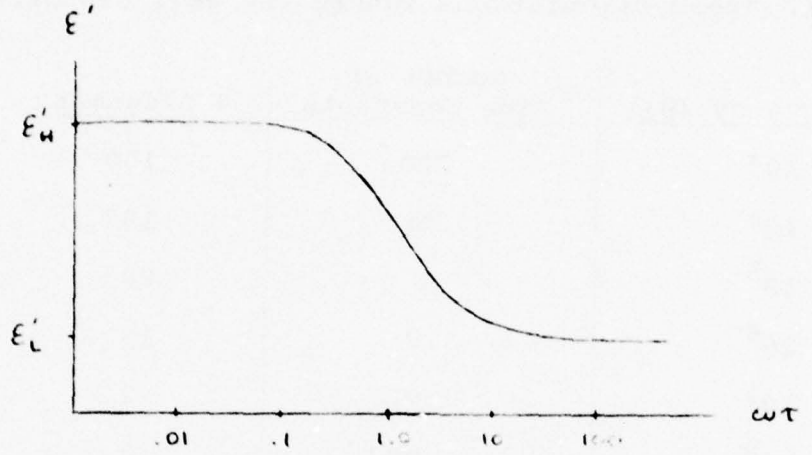

Figure 6. Dipolar polarization. The "L" subscript represents the low frequency limit and the "H" subscript represents the high frequency limit. (From V. V. Daniel, op. cit., p. 17)

at a given temperature (and, therefore, a constant τ). At low frequencies, the period of oscillation of the electric field is relatively high. Thus, the dipoles have a long time to align during each half period, and, as shown in Figure 4, almost all of the dipoles will align during that time. A reasonable value of τ at room temperature is 2.5 μ seconds. At a frequency of 10^3 H_z, the half period of oscillation is .5 seconds. The dipoles therefore have 200 time constants (τ's) in which to align, meaning that roughly only one in 10^{87} will not. At 10^9 H_z (.0002 τ), only .02% will align. Intermediate values are given in

Table 1. These calculations ignore the well distortion

Frequency (H_Z)	Number of Time Constants	% Alignment
10^3	200	~100
10^4	20	~100
10^5	2	86
10^6	.2	18
10^7	.02	2
10^8	.002	.2
10^9	.0002	.02

Table 1. Rough calculations of dipole alignment as a function of frequency.

and the fact that transitions occur both into and out of the site. They are therefore not intended to be quantitatively accurate, but rather to give a general understanding of the quantitative behavior of the dipoles and thereby aid in the qualitative explanation of dipolar polarization.

One very important thing to note in Table 1 is the linearity of the relationship between alignment and number of time constants in the high frequency range. This is expected from a consideration of the mathematical functions used in calculating polarization. From Figure 4, the number of dipoles that align is given by

$$N = N_o (1-e^{-n}) \qquad (10)$$

where n is the number of time constants ($n = t/\tau$). The exponential can be expanded in a Taylor series as follows:

$$e^{-n} = 1 - n + \frac{n^2}{2!} - \frac{n^3}{3!} + \frac{n^4}{4!} - \ldots \qquad (11)$$

when n becomes very small, such as is the case at high frequencies, higher order terms can be dropped.

$$e^{-n} \approx 1 - n \quad , \quad n \ll 1 \qquad (12)$$

Substituting this into equation (10) yields

$$N \approx N_o \ (1 - (1-n)) \ , \ n \ll 1$$

$$N \approx n N_o \quad , \quad n \ll 1 \qquad (13)$$

With this in mind, consider the energy dissipation resulting from the dipole motion. It is a function of the number of dipoles moving per unit time and the resistance to such motion, the latter itself being a function of the material and the temperature. For a given material at a given temperature, the resistance will therefore be a constant. The number of dipoles moving per second is equal to the number of dipoles moving per half period times the number of half periods per second.

$$\sigma'' \propto (N\omega)^x \qquad (14)$$

where x is an arbitrary exponent used for the sake of generality. At very low frequencies, N is high ($\approx N_o$),

but ω is so low that σ'' is very small. As ω increases, N remains near N_o for a while, so σ'' increases as ω^x. As ω continues to increase, N begins to drop significantly, so σ'' increases much more slowly. The high frequency behavior of σ'' is found by substituting equation (13) into equation (14).

$$\sigma'' \propto (n N_o \omega)^x \quad , \text{ high frequencies} \qquad (15)$$

Since n is proportional to the period of oscillation, it is inversely proportional to the frequency.

$$n \propto \frac{1}{\omega} \qquad (16)$$

Substituting this into equation (15) yields

$$\sigma'' \propto N_o^x \qquad (17)$$

which shows that σ'' becomes constant at high frequencies. Intuitively, the decrease in motion per cycle is compensated by the increase in cycles per second. σ'' is plotted in Figure 7.

Figure 7. Frequency dependence of dielectric conductivity. Specific values are omitted because they depend on many other factors. Only the form of the function is of interest here.

Since we know the relationship between σ'' and ε'', we can now describe the frequency dependence of ε''. Recall equation (5)

$$\varepsilon'' = \frac{\sigma''}{\varepsilon_0 \omega}$$

Like σ'', ε'' starts out very low, then increases according to ω^{x-1} (whereas σ'' increased according to ω^x). As σ'' begins to steady out, ε'' will peak and decrease as $1/\omega$. This is shown in Figure 8.

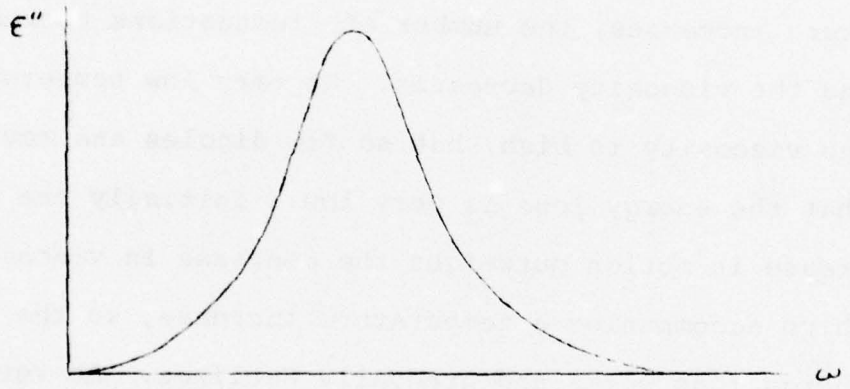

Figure 8. Frequency dependence of the imaginary component of the complex dielectric constant.

D. Temperature Dependence

Temperature affects energy dissipation through two mechanisms--the number of dipoles undergoing site transitions and the resistance to the dipole motion. The viscous fluid model provides a good representation of the dielectric for these functions. Imagine the

material to be a viscous fluid containing the fluctuating dipoles. The energy loss in this model is a function of the dipole motion and the fluid viscosity. High energy loss corresponds to a lot of motion and high viscosity. The velocity of the ions during fluctuations is assumed to be constant, so temperature affects dipole motion only by affecting the number of dipoles undergoing the motion. As temperature increases, the number of fluctuations increases, and the viscosity decreases. At very low temperatures the viscosity is high, but so few dipoles are moving that the energy loss is very low. Initially the increase in motion outweighs the decrease in viscosity which accompanies a temperature increase, so the energy loss peaks and gradually declines. At very high temperatures, there is a lot of motion, but the viscosity is so low that the energy loss is very low. In reality the viscosity corresponds to the relaxation time, and the number of dipoles moving is given by equation (10).

$$\tau = \tau_o e^{E/kT} \qquad \text{(viscosity)}$$

$$N = N_o (1-e^{-n}) \qquad \text{(motion)}$$

where

$$n = \frac{t}{\tau} = \frac{\frac{1}{2}(1/\omega)}{\tau_o e^{E/kT}} = \frac{e^{-E/kT}}{2\tau_o \omega} \qquad (18)$$

Thus, with regard to temperature dependence, this model predicts that viscosity is an exponential and motion is an exponential of an exponential. The latter dominates at low temperatures, and the former at high temperatures. This is shown in Figure 9.

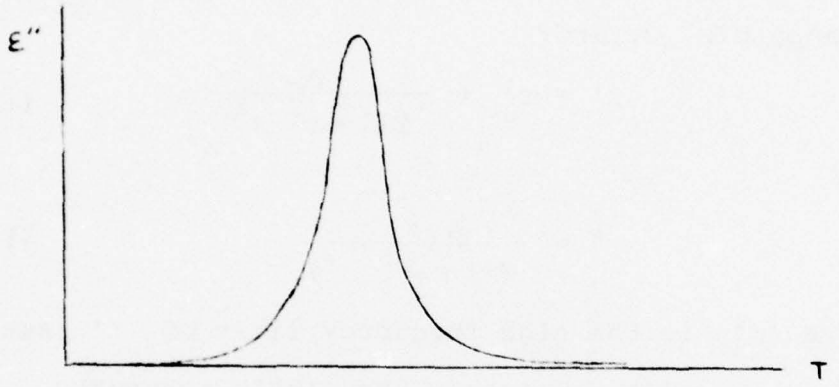

Figure 9. Temperature dependence of the imaginary component of the complex dielectric constant.

The exact location and shape of the peak depend on the activation energy (E), the characteristic relaxation time (τ_o), the frequency (ω), and the various proportionality parameters such as total number of dipoles (N_o), dipole strength, etc.

E. Debye Equations

Now that each factor affecting the dielectric constants has been examined individually in depth, it is possible to tie them all together into a unified

form. This is done in the Debye equations, in which the real and imaginary dielectric constants are given as a function of temperature, frequency, and all other system parameters. These equations, which are derived in a similar form using an electrical circuit analogy in Appendix 2, are:

$$\varepsilon' = \varepsilon'_H + \frac{A}{T(1 + \omega^2 \tau^2)} \qquad (19\text{-a})$$

and

$$\varepsilon'' = \frac{A\omega\tau}{T(1 + \omega^2 \tau^2)} \qquad (19\text{-b})$$

where ε'_H is the high frequency limit of ε' (see Figure 6) and A represents the dipole strength.

$$A = \frac{Np^2}{3\varepsilon_0 k} \qquad (20)$$

where N is the dipole concentration and p is the dipole moment. The plots of these are three dimensional graphs whose cross sections are the same as the frequency and temperature dependence plots shown earlier in this paper. ε' and ε'' are related to each other through the equation

$$\varepsilon'' = \frac{\varepsilon' G}{C\omega} \qquad (21)$$

where G is the conductance (reciprocal of resistance) of the material. This section is concluded by noting that the simple dipole model and the Debye equations

predict a single peak spectrum for ε".

F. Measured Spectra

The previously mentioned inadequacy of the simple dipole model will now be demonstrated by examining some of the experimental measurements which have been made on non-radiated crystals. For example, consider the dielectric spectrum of .1% erbium doped calcium fluoride at 100 Hz, shown in Figure 10. There is a considerable difference between it and the single

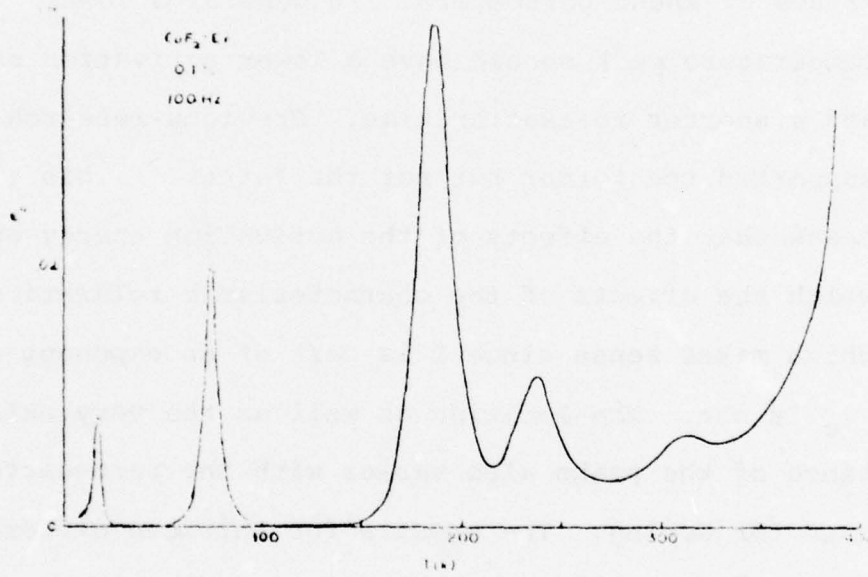

Figure 10. CaF_2: Er, 0.1 mol - %, 100 Hz

peak that was theoretically predicted; however, the basic peak structure is present. Each peak is designated by a relaxation number ($R_2 - R_1$). The argument that will be advanced in this paper is that each peak corresponds to a different charge configuration (or different ion motion within the same charge configuration). Each configuration has a characteristic relaxation time (τ_o) and activation energy (E). The temperature location of a given peak depends on the values of these parameters. In general a lower temperature peak should have a lower activation energy and a shorter relaxation time. Previous research has supported the former but not the latter.[5] This just means that the effects of the activation energy outweigh the effects of the characteristic relaxation, which makes sense since E is part of an exponent and τ_o is not. The location as well as the very existence of the peaks also varies with the rare-earth used for doping. The spectra for thirteen different rare-earths are shown in Figure 11. Atomic number decreases from top to bottom and left to right. Two important trends are demonstrated: R_4 and R_5 occur at lower temperatures as atomic number decreases, and

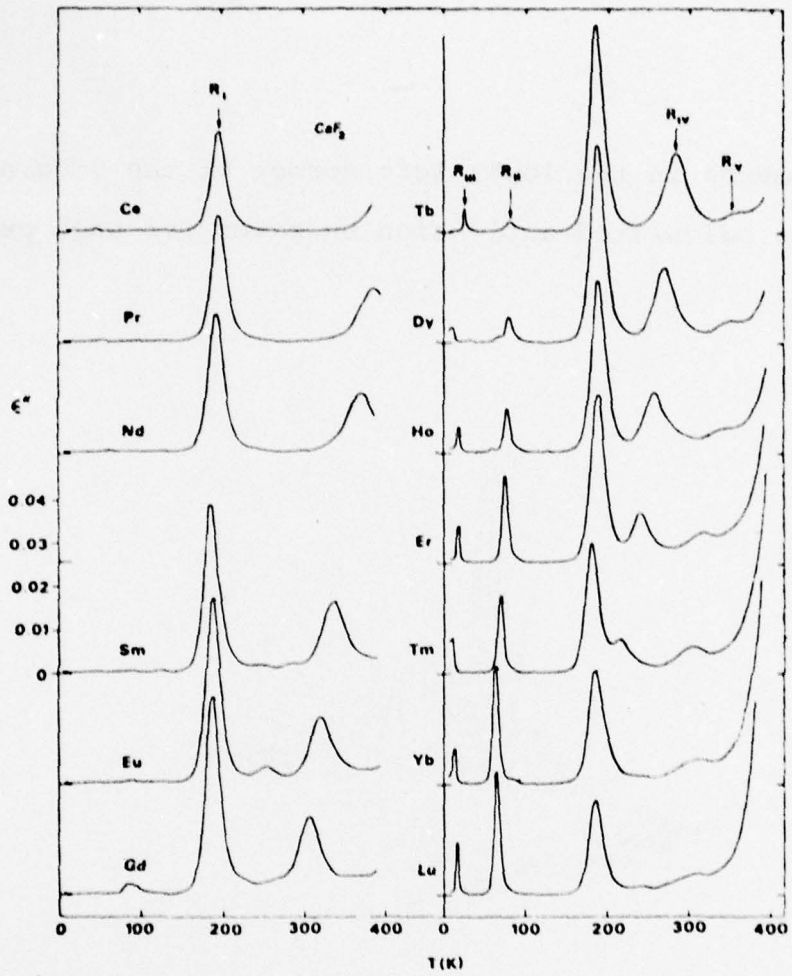

Figure 11. The dielectric spectra of calcium fluoride doped with thirteen different rare-earths.

R_2 and R_3 decrease in size and eventually disappear as atomic number increases. One other interesting plot to study is that of doping concentration dependence shown in Figure 12. R_1, R_4, and R_5 grow with concentration, and R_1 and R_2 grow to a peak then decrease.

The numbers in the lower left corner of the diagram are the calculated activation energies for each peak.

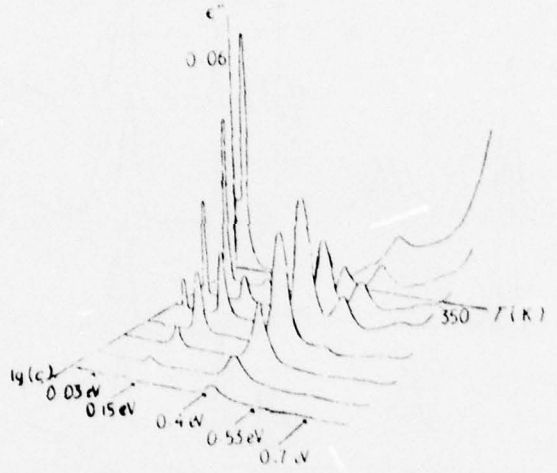

Figure 12. ε" as a function of temperature and concentration in erbium doped calcium fluoride. The concentration ranges from .001% to 3%.

Although the scientific community still does not know the specific nature of the peaks, the author supports the following hypothesis: R_1 is from the simple dipole; R_2 is from a relatively simple cluster; and R_3, R_4, and R_5 are from larger and more complex clusters. At very low concentrations, almost no

clusters exist and there is only a small R_1 peak from the small number of dipoles that exist. As the concentration increases, the number of dipoles increases and some simple clusters begin forming. Hence, R_1 and R_2 increase. As the concentration continues to increase, larger clusters form, so R_3, R_4, and R_5 begin to grow. Also, other rare-earths attach themselves to the simple dipoles and clusters of R_1 and R_2, so these two peaks gradually decrease. At high concentrations, almost all the rare-earths are part of clusters. R_1 and R_2 are very small whereas R_3, R_4, and R_5 are now large, with R_3 being very large. As for the clusters themselves, some general concepts will be discussed here. First, a cluster need not necessarily be balanced in charge. The crystal as a whole is, but one cluster could have excess fluorines and another could have a shortage. Secondly, fluorine motion in a cluster should only occur between equivalent sites (sites with the same potential energy). In the bistable model (Figure 3) the two well depths are the same when unaffected by an electric field. If they were not, the ions would migrate to one site and stay there (unless the electric field were strong enough to overcome the potential difference, in which case transitions will

occur). Equivalence is generally attained through symmetry. For example, consider the cluster in Figure 13. Because of the simple direct fluorine

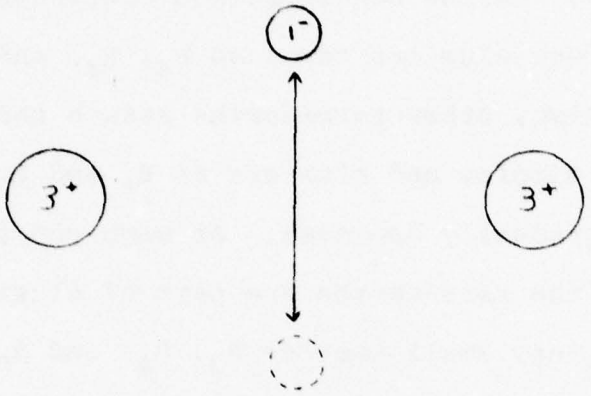

Figure 13. A simple cluster consisting of two rare-earths and one interstitial fluorine. The fluorine sites are potentially equivalent because of symmetry.

motion and the Coulomb force attracting the fluorine to the center, such a cluster would probably have a low activation energy. It is also possible that a fluorine could transit between sites in different clusters, as shown in Figure 14. This transition is considerably more complicated than it appears, though,

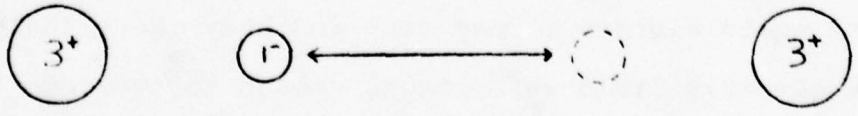

Figure 14. Site transition between clusters.

because of the existence of calcium ions between the clusters. These examples are only hypothetical and are intended to give a general understanding of clusters and their motion. The important point to conclude dielectric theory with is that there is an extremely large number of possible clusters and motions, and no one yet knows which are responsible for the observed dielectric spectra. This study should provide additional insights.

III. EXPERIMENT

The crystals in this study were obtained in their raw form from Optovac, Inc. They were then cut, ground, and polished, the final product being 25.4 mm in diameter and 1.5 mm thick. Aluminum electrodes were then evaporated onto both sides of each crystal. Good evaporations were insured by thoroughly cleaning the crystal surfaces with freon and by conducting several minutes of ion discharge after bleeding argon into the vacuum chamber. Edge effects are eliminated by using three terminal capacitance. This is illustrated in Figure 15. During evaporation of one of the

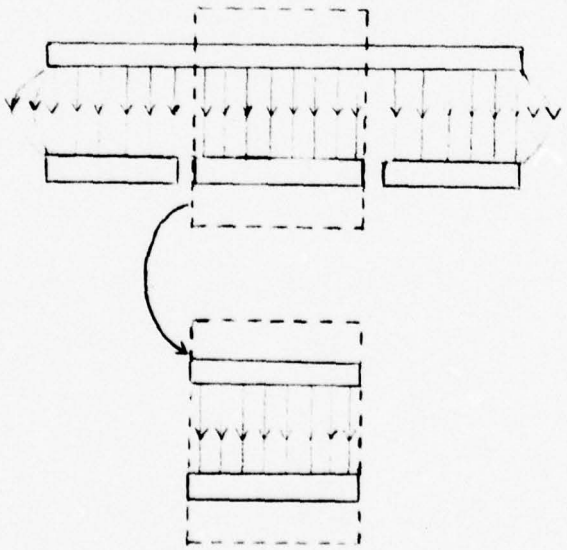

Figure 15. Three terminal capacitance used to eliminate edge effects.

sides of the crystal, a thin shadow ring is centered on the crystal and held in place by a magnet under the crystal. This protects the area under it from the evaporation and creates a small gap (not more than .01 mm wide) in the electrode surface. The readings are taken from the inner area only, for which there are no edge effects.

Temperature control from 5°K to 380°K is accomplished in a Cryogenics Associates CT-14 cryostat. The system uses liquid nitrogen for temperatures down to 77°K and liquid helium for temperatures down to 5°K. Fine adjustments and higher temperatures are attained with a heater delivering up to 16 watts. The temperature is measured by matching the resistance of temperature sensitive resistors in a bridge circuit. Because of the sizes of their resistance gradients, Germanium is used for very low temperatures and Platinum for higher temperatures.

The actual dielectric measurements are taken using a General Radio 1615 Capacitance Bridge. The bridge measures C and G/ω and operates at 5 audio frequencies: 10^2, $10^{2.5}$, 10^3, $10^{3.5}$, and 10^4. A detailed explanation of the bridge circuit and its principles of operation are included in Appendix 3.

The accuracy of the instrument is extremely high, being better than 1 part per million (ppm). To calculate ε' from C is a simple matter of knowing the geometry of the capacitor.

$$\varepsilon' = \frac{C}{C_0} = \frac{Cd}{\varepsilon_0 A}$$

where d is the distance between the plates and A is the plate area. Unfortunately, though, this calculation is complicated by the fact that the capacitor dimensions change with temperature. The formula for ε' at temperature T, which is derived in Appendix 4, is therefore

$$\frac{\varepsilon'_T}{\varepsilon'_{300}} = \frac{C_T}{C_{300}} e^{-\int_{300}^{T} \alpha_p dT} \qquad (22)$$

where α_p is the isobaric linear thermal expansion coefficient and the subscripts indicate the temperature at which the value of the parameter is taken. The values of α_p are those for pure calcium flouride because of a lack of values for rare-earth-doped samples; however, given the doping concentrations used and the nature of thermal expansion, the difference should be negligible. The exponent was evaluated using numerical integration. Finally, ε'' is calculated from Equation 21 ($\varepsilon'' = \varepsilon' G/\omega C$), where G/ω is the value given

by the bridge and ε' and C are known from the previous calculations.

The procedure in this experiment was to record the dielectric spectrum as a function of temperature at each of the 5 frequencies both before and after radiation in order to determine the effects of the radiation. Two types of radiation were tested: neutron and gamma rays. The neutron sources were the sub-critical reactor and the 14 MeV neutron generator at the Academy. The gamma ray source was a Co^{60} source at the Naval Research Laboratory in Washington, D. C. Co^{60} provides 1.17 MeV and 1.33 MeV gamma rays.

IV. RESULTS

A. Neutron Radiation

The results of neutron radiation were somewhat disappointing in that the dielectric spectra were statistically the same before and after exposure. The following crystals were tested using the neutron generator: pure Calcium Fluoride, four rare earths (Cerium, Neodymium, Praseodymium, and Gadolinium), and two alkali metals (Lithium and Cesium). Holmium was tested using the sub-critical reactor. The pure crystal was tested as a control to insure that any observed effects were the result of changes having to do with the dopant rather than disruptions of the crystal lattice structure itself. The alkali metals were tested for general interest and comparative purposes. The only effects that were observed were in Lithium, but they were sporadic and believed to be caused by improper loading (poor electrical contact between the evaporated electrodes and the bridge circuit). Subsequent testing of an irradiated Lithium doped crystal found no effects. The Gadolinium sample was irradiated, but it shattered in the high velocity compressed air exit tube of the neutron generator; hence, dielectric measurements were not possible.

B. Gamma Radiation

In contrast to the neutrons, gamma-rays produced dramatic results. For the sake of clarity, only characteristic results will be given here. The remainder of the results are given in Appendix 1 and will be referred to. Figure 16 shows the pre and post radiation dielectric spectra of 0.1% Holmium doped CaF_2 at 1000 Hz. The radiation increased R_1 and R_2, decreased R_3 and R_4, and, most interestingly, induced a new relaxation between R_2 and R_3 at approximately 56 °K. There is also a small effect at approximately 150 °K. The crystal was exposed to the cobalt source for 100 minutes, making the total dose 1.86×10^6 R. Crystals doped with 0.1% Cerium, Lutetium, Samarium, Terbium, Thulium, Lanthanum, and Yttrium were also exposed to this same dose.[6] Their spectra (shown in Appendix 1) reveal that low temperature relaxation inducement also occurred in Samarium, Cerium, Thulium, Terbium, Lanthanum, and Yttrium. Only Lutetium did not undergo a significant change. Because of the size and form of its induced peaks, Samarium was chosen for further study. This further study will include data on the effects of doping concentration, radiation dose, and time. Figure 17 gives the pre and post radiation

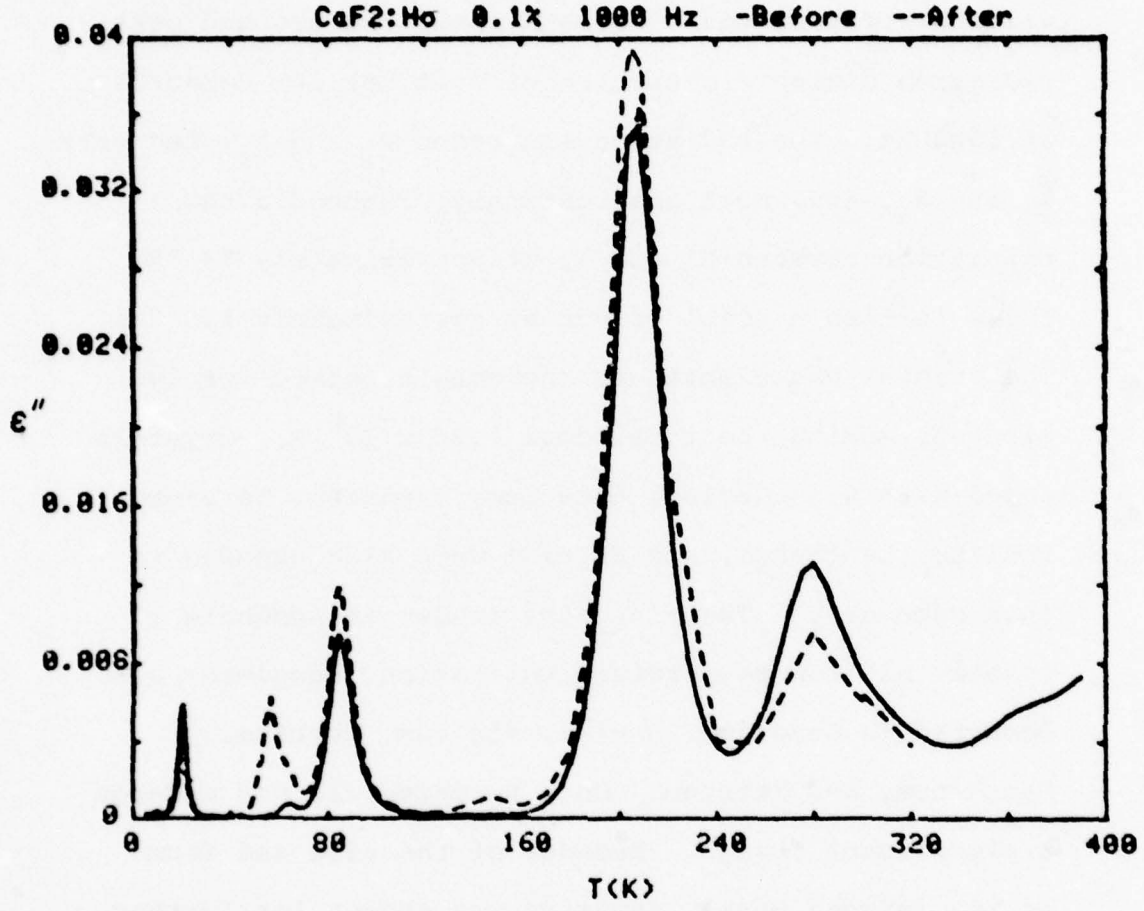

Figure 16. Pre and post radiation dielectric spectra of 0.1% Holmium doped CaF_2 at 1000 Hz.

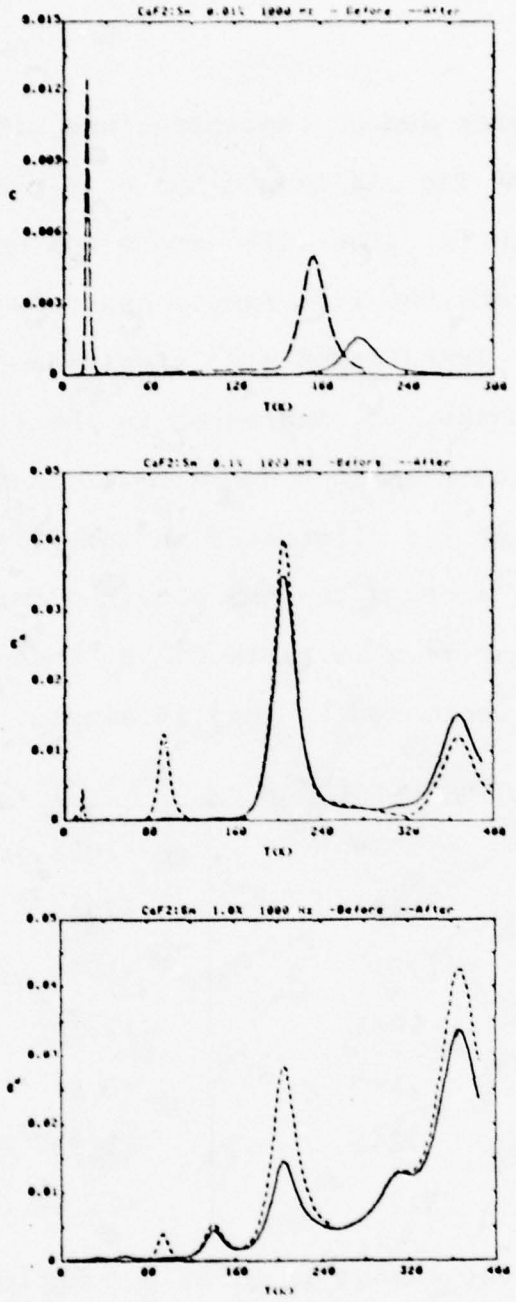

Figure 17. Pre and post radiation spectra for three concentrations of Samarium doping: (a) .01%; (b) .1%; (c) 1%. Total dosage was 2.12×10^6 R. Note the different scale used in (a).

spectra for three doping concentrations of Samarium (.01, .1, 1%). The .1% sample has a 16 and a 94 °K peak induced in it. The .01% sample has only the 16°K peak induced, and the 1.0% sample has only the 94 °K peak induced. Irradiation also significantly changed the existing peaks. R_1 increased in the 1% and .1% samples and either shifted 30 °K lower in temperature and increased or was eliminated in the .01% sample. These results, along with some obtained for Erbium, are given in tabular form in Table 2. R_4 increased in the 1% sample and decreased in the .1% sample.

Dopant:	concentration	R_1
Sm:	.01%	-100% or shift
	.1%	+20%
	1.0%	+100%
Er:	.03%	+2.1%
	.1%	+2.6%
	.3%	+11.3%
	1.0%	+11.6%

Table 2. Percent change in R_1 as a function of concentration.

Dose effects were studied by irradiating .1% Samarium samples for three different time lengths: 1, 2, and 4 hours (1.06×10^6, 2.12×10^6, and 4.24×10^6 Roentgens, respectively). The percentage increase or

decrease in the peak heights for R_1 and R_4 (the only two pre-existing peaks) is given in Table 3.

Radiation Time	Dose	R_1	R_4
1 hour	1.06×10^6 R	+12.4%	-18%
2 hours	2.12×10^6 R	+20%	-18.3%
4 hours	4.24×10^6 R	+23%	-22%

Table 3. Percent change in R_1 and R_4 as a function of radiation dose for .1% Sm: CaF_2.

The initial height of the radiation induced peak at 94 °K also varied with dosage, as shown in Table 4. This table lists the peak height bridge readings (G/ω) as a function of dose.

Radiation Time	Initial Induced Peak Height
1 hour	699
2 hours	748
4 hours	934

Table 4. Induced peak height as a function of radiation dose in .1% Sm: CaF_2 .

ε'' is proportional to G/ω by a factor of ε'/C (Equation 21), which, at a given temperature, is a constant. Therefore, the differences between the peak heights in the table are proportionally the same as those for

the actual values of ϵ''. As both these tables demonstrate, the changes do increase as dose increases, but at a diminishing rate. These values are thus indicative of an exponential function.

The stability of these changes (time effects) was carefully studied in a .1% Samarium doped crystal which had been irradiated for 4 hours. Table 5 lists the bridge readings (G/ω) for each peak height at approximate times after the initial measurement.

Time	R_1	R_2	16.5 °K	94 °K
pre-radiation	3234	790	0	37
initial	3681			934
8 hours	3837	617	400	1113
18 hours	3912	616	372	1018
22 hours	3950	615	361	955
45 hours	3974		324	912

Table 5. Time dependence of radiation effects in .1% Sm: CaF_2 following a dose of 4.24×10^6 R.

Continuing measurements are showing that R_1 remains constant within statistical fluctuations around 3960, and the two radiation induced peaks are continuing to decay exponentially. Further data on R_4 is not yet available, but it appears to have reached its

steady state value very quickly. Plots of the percent change in R_1 and the absolute height of the induced peak as a function of time are shown in Figures 18 and 19, respectively.

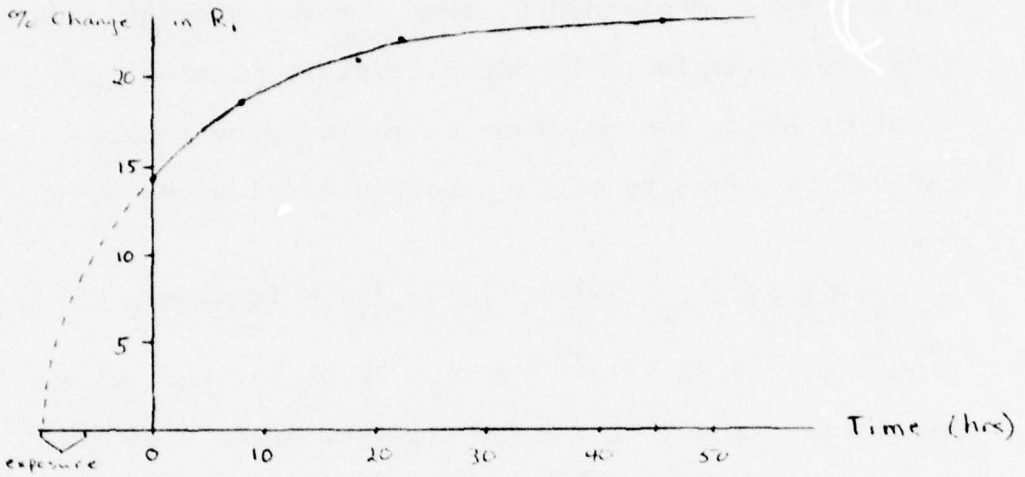

Figure 18. Percent change in R_1 vs. time.

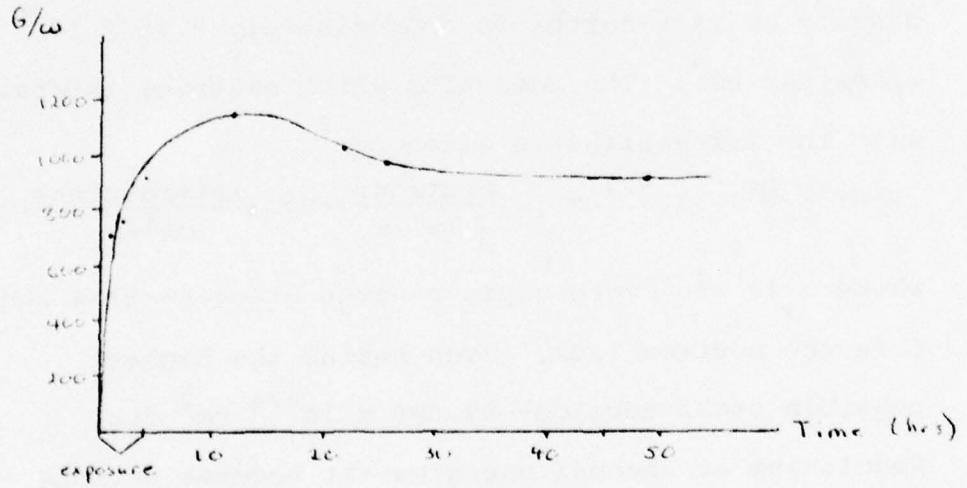

Figure 19. 94 °K induced peak height vs. time.

V. DISCUSSION OF RESULTS

A. Neutrons

The lack of any effects from neutron radiation can be easily explained by some simple calculations. Take, for example, a 1% doped crystal, meaning that 1 out of every 100 calciums is replaced by a rare-earth. The density of CaF_2 molecules is given by the formula:

$$N=N_0\left(\frac{\text{molecules}}{\text{mole}}\right)\frac{1}{MW}\left(\frac{\text{moles}}{\text{gm}}\right)\rho\left(\frac{\text{gm}}{\text{cm}^3}\right)=\frac{N_0\rho}{MW}\left(\frac{\text{molecules}}{\text{cm}^3}\right). \quad (23)$$

Plugging in 6.02×10^{23} for N_0, 78.08 for the molecular weight, and 3.18 for the density gives 2.45×10^{22} molecules per cm^3. Since there is one calcium per molecule and one rare-earth per 100 calciums, the density of rare-earths is approximately 2.45×10^{20} atoms per cm^3. The rate with which neutrons interact with the rare-earths is given by

$$R=N\left(\frac{\text{atoms}}{\text{cm}^3}\right)\sigma\left(10^{-24}\text{cm}^2\right)\phi\left(\frac{\text{neutrons}}{\text{cm}^2\text{-s}}\right)=N\sigma\phi\left(\frac{\text{interactions}}{\text{cm}^3\text{-s}}\right) \quad (24)$$

where σ is the microscopic neutron cross section and ϕ is the neutron flux. Even taking the highest possible cross section--$49{,}000 \times 10^{-24}$ cm^2 for Gadolinium at thermal energies--it becomes obvious that R is extremely low. Plugging in N and σ yields

$$R(Gd) = 12\phi \ . \quad (25)$$

The highest possible thermal flux that could be arranged from either the sub-critical reactor or the neutron generator is well below 10^6; but even using this value, the interaction rate would be 1.2×10^7 interactions per cm^3 per second, or 4.3×10^{10} interactions per cm^3 per hour. Dividing this by the rare-earth ion density shows that exposure for one hour would result in an interaction with less than one fifty-millionth of one percent of the rare-earths. Higher energy neutrons give higher fluxes, but the cross sections are much smaller at these energies.

B. Gamma Rays

The most important information revealed by this study is that highly concentrated energy in the form of gamma rays significantly affects the dielectric properties of the materials studied. No changes were found in a pure calcium fluoride crystal which was irradiated by gamma rays (in addition to the one irradiated with neutrons); therefore, the effects are related to the rare-earth dopant. This result supports the cluster hypothesis in that such concentrated energy could easily change the nature and organization of clusters within the material. Take, for example, the quadropole shown in Figure 20. Such a charge

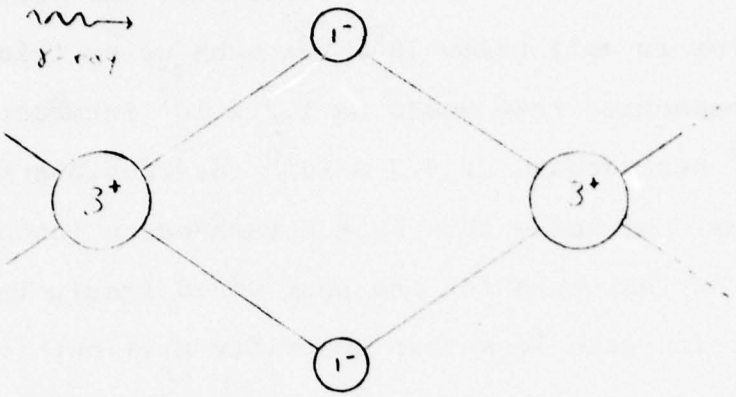

Figure 20. Two rare-earths and two interstitial fluorines together, forming a quadropole.

configuration could not polarize in the sense that a dipole does, because there are no open equivalent sites. If, however, a gamma ray interacted with one of the fluorines in such a way as to make it leave the configuration, there would be an open equivalent site. This is exactly the cluster that is shown in Figure 13. As previously indicated, such a cluster should have a low activation energy, causing it to peak at a low temperature. It could, therefore, be one of the radiation induced peaks, or perhaps the R_2 peak (which radiation generally tended to increase). Indeed, it is possible that the 94°K induced peak in Samarium is an R_2 peak. Current nuclear magnetic resonance studies have in fact confirmed the existence

of this charge configuration in rare-earth doped calcium fluoride (Ytterbium and Erbium).[7]

The final point of discussion involves the stability of the induced effects. Changes in the pre-existing peaks are stable, whereas peaks that were completely induced slowly decay back to zero. Measurements taken on an Erbium sample irradiated a year prior to the beginning of this study showed that the induced low temperature peak had disappeared. What this indicates is that some clusters are stable and some are not. Those that are stable exist naturally, and those that are unstable can only be induced by some means such as radiation. Take the .1% Samarium sample that was exposed for four hours as an example. The following scenario is a possible explanation of what happened during and after radiation. The gamma rays broke up some of the R_4 clusters, causing this peak to immediately decrease to its steady state value. They also broke up some complex clusters which either didn't have peaks or had them outside the temperature range of this study. These are all very stable. The "loose" ions freed by this process gradually form into dipoles or simple clusters. This increases R_1 (the dipoles) and creates

new peaks (from clusters which had not previously existed). At the moment the crystal is removed from the radiation, the ions are still forming new dipoles and clusters, so these peaks continue to increase temporarily. However, the induced clusters themselves are not stable, or at least not as stable as other possible configurations, so they slowly form into very stable clusters which, again, either do not produce peaks or produce them outside the temperature range. These could very well be the same clusters that existed before irradiation. Thus, R_1, which is caused by stable dipoles, remains at its increased value; R_4 remains at its decreased value; and the induced peaks decay back to zero. The stability of a particular cluster depends on the rare-earth, as is evidenced by the fact that the heavier rare-earths do not have naturally occurring low temperature peaks (see Figure 11).

C. Applications

Although the primary importance of this study is the addition of important information on a subject that is not yet well understood by the scientific community, it may have more direct application in radiation dosimetry If a particular effect can be calibrated as a function of

radiation dose, then use of a dielectric crystal as a dosimeter is possible. The particular effect could be moved to room temperature by adjusting the frequency, since an increase in frequency increases the temperature at which a peak will occur. Low dosage studies will have to be done to investigate this possibility though, because the doses used in this study would result in certain death.

VI. SUMMARY AND CONCLUSION

1. Effects of Co^{60} gamma-rays on rare-earth doped CaF_2 depend strongly on the dopant concentration.

2. Effects on 0.1% samples depend on the particular dopant, but in general they are typified by the effects on holmium which are:
   A. Increase R_1
   B. Increase R_2
   C. Decrease R_3
   D. Decrease R_4
   E. Create a relaxation between R_2 and R_3.

3. Radiation effects increase as dose increases, but they do so at a diminishing rate.

4. Changes in existing peaks are stable, whereas new peaks generally decay very slowly to zero.

5. These results are entirely consistent with the cluster hypothesis explained in this paper. Specifically, R_1 comes from dipoles, R_2 from simple clusters, and R_3, R_4 and R_5 from more complex clusters.

FOOTNOTES

1. John Fontanella and Carl Andeen, Journal of Physics C: Solid State Physics, 1055 (1976).

2. J. P. Scott and J. H. Crawford, Jr., Physical Review Letters 26, 384 (1971); Physical Review B 4, 668 (1971).

3. A. D. Franklin, J. M. Crissman, and K. F. Young, Journal of Physics C: Solid State Physics 8, 1244 (1975).

4. C. Andeen, D. Link, and J. Fontanella, Physical Review B 16, 3762 (1977).

5. C. Andeen, D. Link, and J. Fontanella, op.cit., 3764.

6. Yttrium is not a rare-earth element. However, it is trivalent and has a comparable ionic radius, so it was tested for comparative purposes.

7. R. J. Booth, D. R. McGarvey, and M. R. Mustafa (to be published), Physical Review.

REFERENCES

1. Daniel, Vera V. Dielectric Relaxation. New York: Academic Press, 1967.

2. Kittel, Charles. Introduction to Solid State Physics. New York: John Wiley and Sons, 1971.

3. A. D. Franklin, J. M. Crissman, and K. F. Young, Journal of Physics C: Solid State Physics 8, 1244 (1975).

4. C. Andeen, D. Link, and J. Fontanella, Physical Review B 16, 3762 (1977).

5. C. Andeen, D. Link, and J. Fontanella, op.cit., 3764.

6. R. J. Booth, D. R. McGarvey, and M. R. Mustafa (to be published), Physical Review.

APPENDIX I

PRE AND POST RADIATION SPECTRA

Here the plots of the results of those dopants which were not included in the text are given. They are: Cerium, Lutetium, Terbium, Thulium, Lanthanum, and Yttrium. All samples are 0.1% and measured at 1000 Hz.

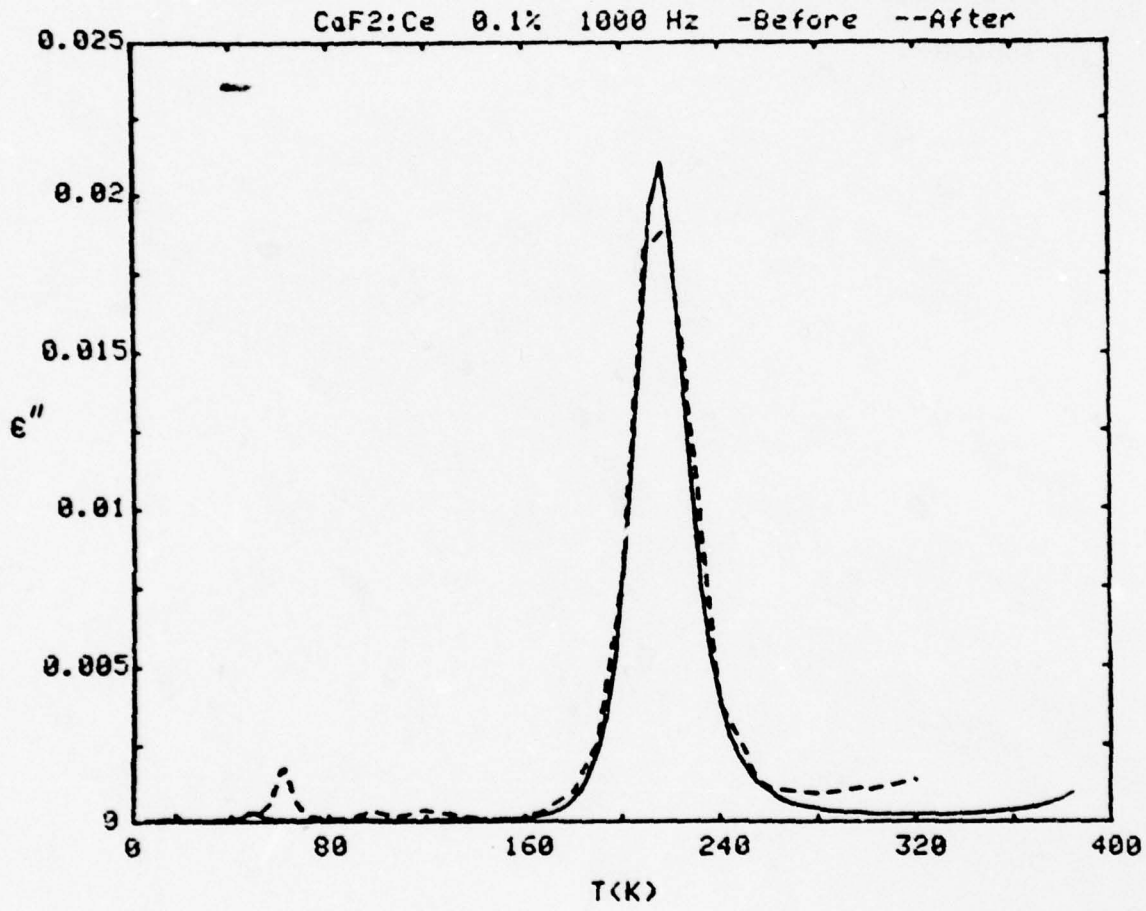
CaF2:Ce 0.1% 1000 Hz -Before --After
0.025
0.02
0.015
ε"
0.01
0.005
0
0
80
160
240
320
400
T(K)

Cerium

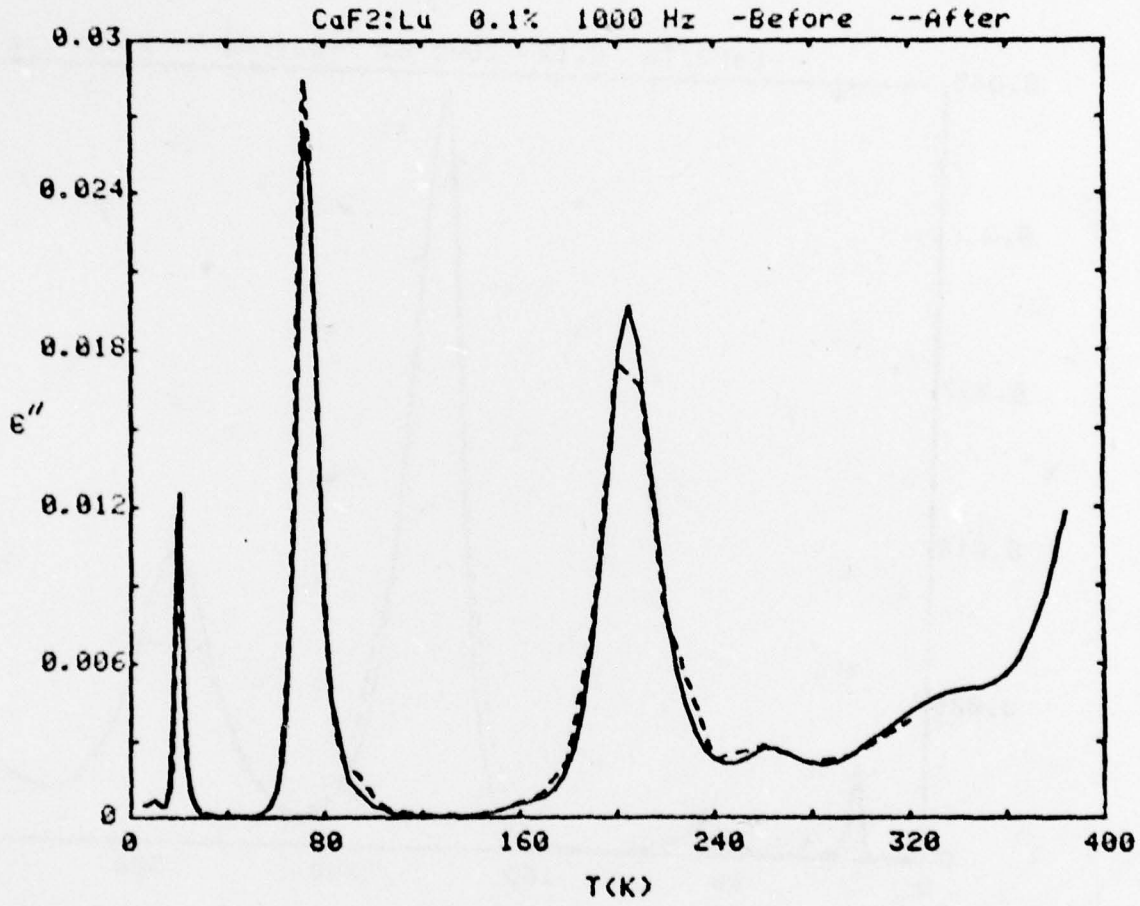
CaF2:Lu 0.1% 1000 Hz -Before --After
0.03
0.024
0.018
ε″
0.012
0.006
0
0
80
160
240
320
400
T(K)

Lutetium

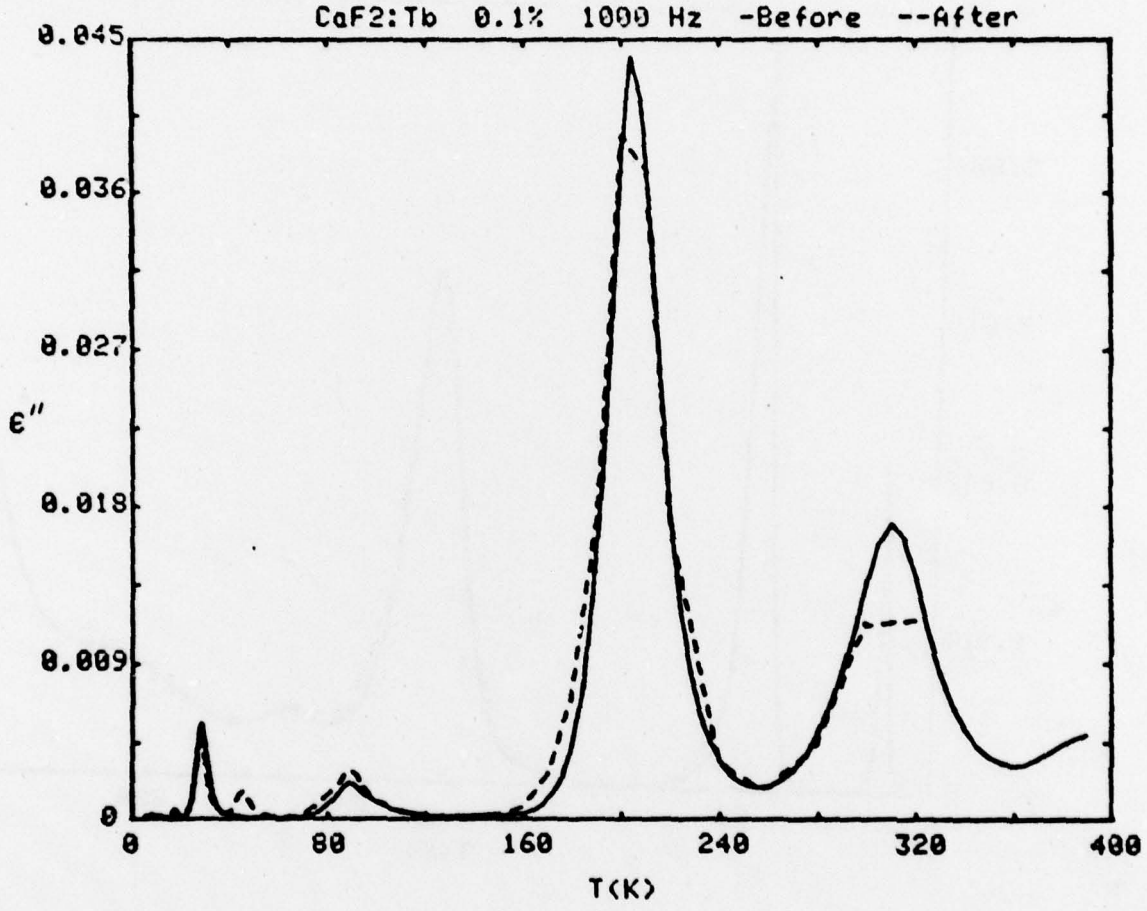
CaF2:Tb 0.1% 1000 Hz -Before --After
0.045
0.036
0.027
ε″
0.018
0.009
0
0
80
160
240
320
400
T(K)

Terbium

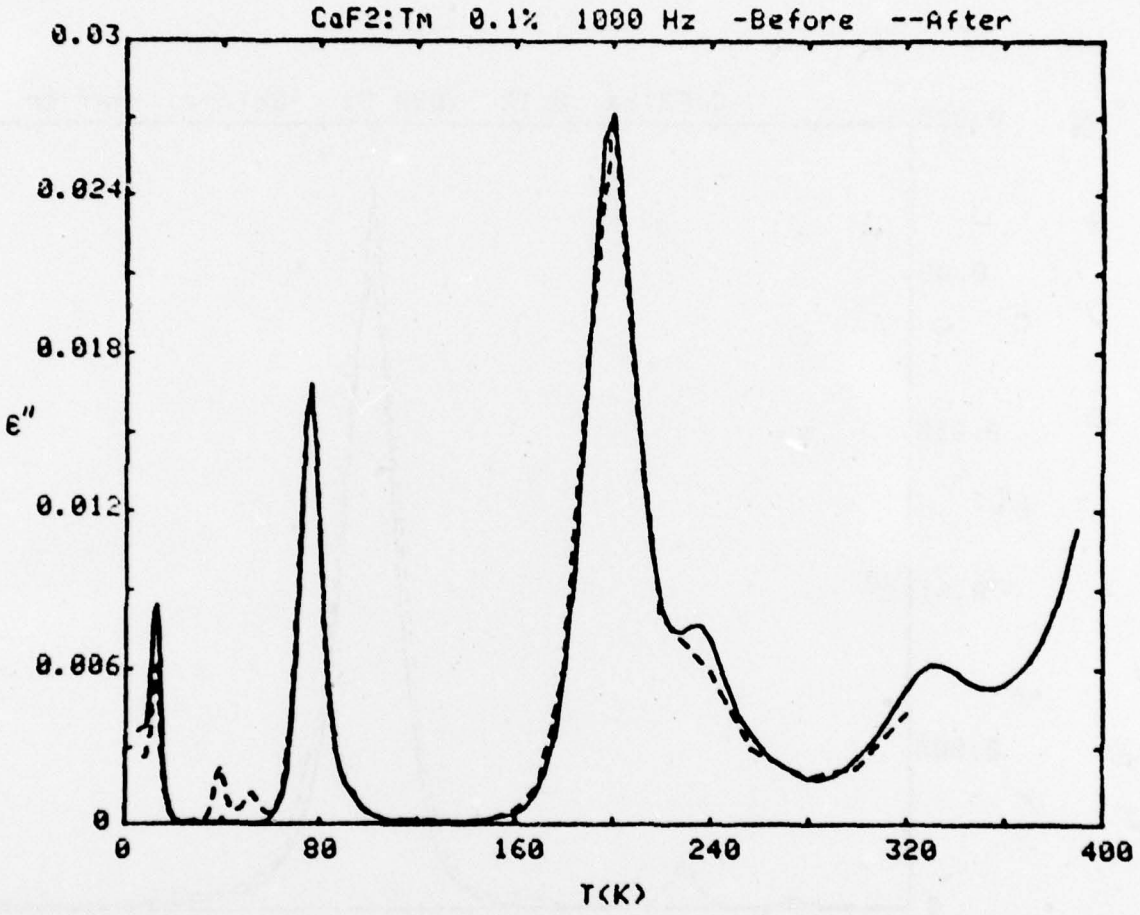
CaF2:Tm 0.1% 1000 Hz -Before --After
0.03
0.024
0.018
ε"
0.012
0.006
0
0
80
160
240
320
400
T(K)

Thulium

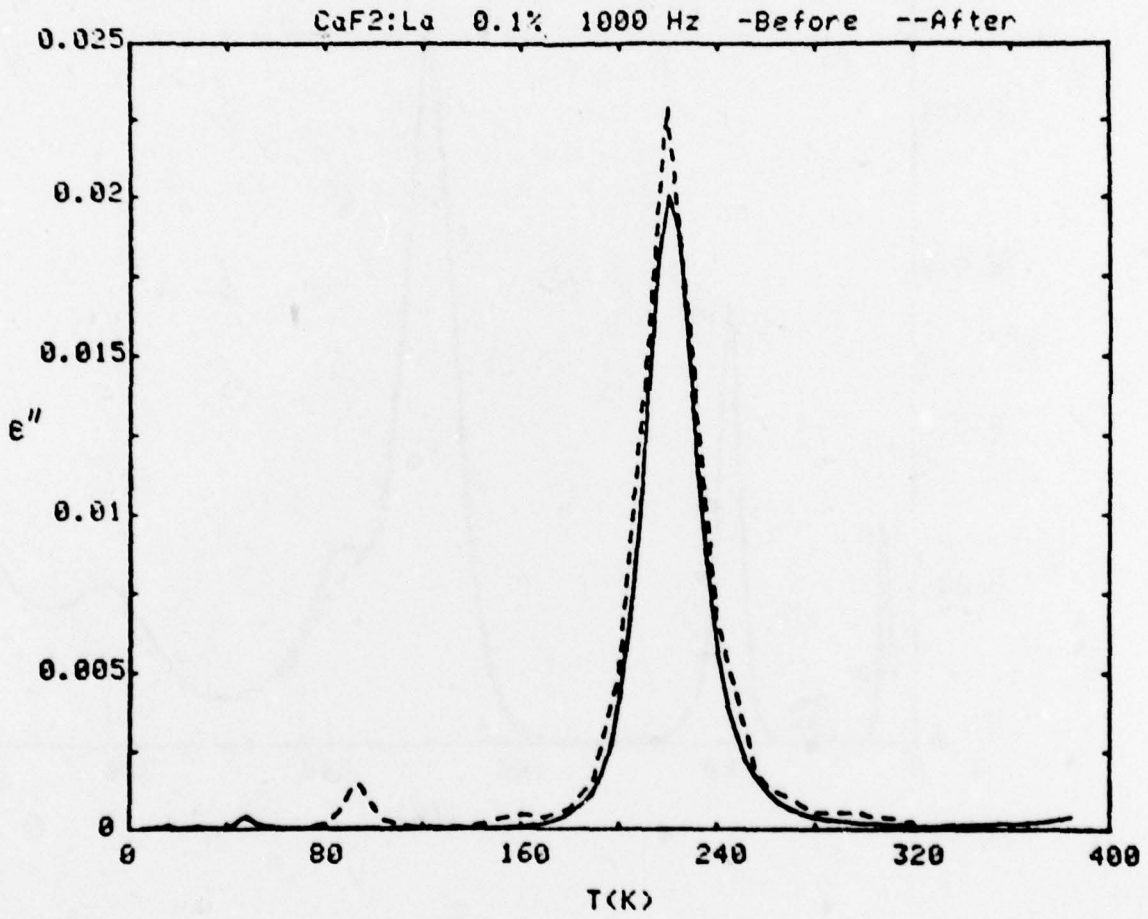
CaF2:La 0.1% 1000 Hz -Before --After
0.025
0.02
0.015
ε″
0.01
0.005
0
0
80
160
240
320
400
T(K)

Lanthanum

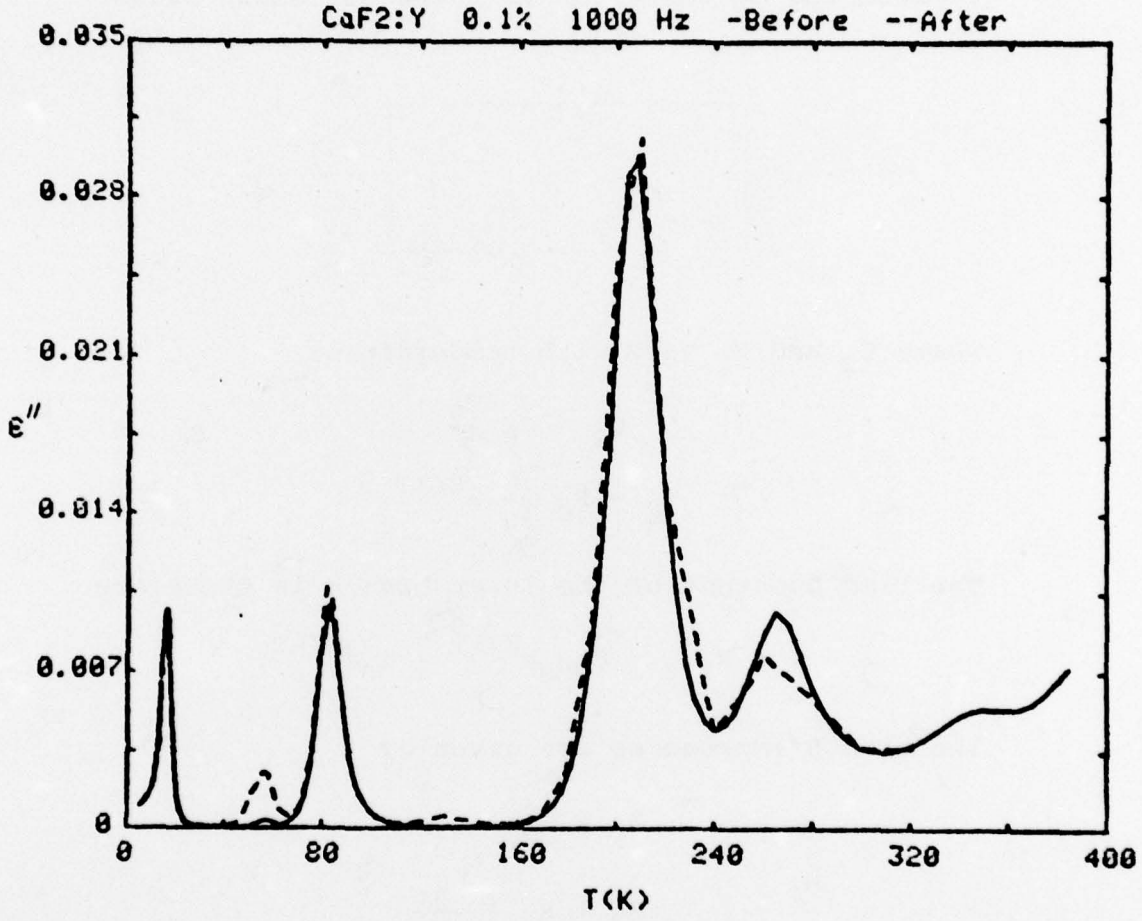
CaF2:Y 0.1% 1000 Hz -Before --After
0.035
0.028
0.021
ε″
0.014
0.007
0
0
80
160
240
320
400
T(K)

Yttrium

APPENDIX II

ELECTRIC ANALOGY: DERIVATION OF THE DEBYE EQUATIONS

The electrical properties of a dielectric can be represented by the electrical circuit shown below.

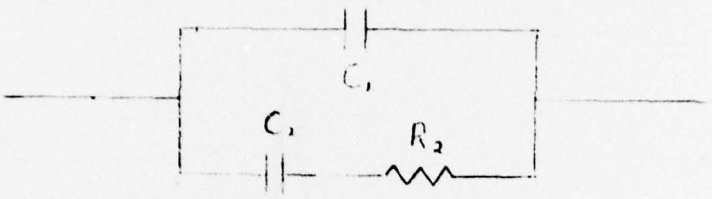

where C_2 and R_2 vary with temperature:

$$C_2 = C_0 \frac{T_0}{T}$$

$$R_2 = R_0 \frac{T}{T_0} e^{E/kT}.$$

The time constant of the lower branch is therefore

$$\tau = R_2C_2 = C_0R_0e^{E/kT} = \tau_0e^{E/kT}.$$

The branch impedances are given by

$$Z_1 = \frac{j}{\omega C_1}$$

$$Z_2 = R_2 + \frac{j}{\omega C_2}$$

$$\frac{1}{Z_T} = Y_T = \frac{1}{Z_2} + \frac{1}{Z_1}$$

$$Y_T = \frac{1}{R_2 + \frac{j}{\omega C_2}} - j\omega C_1 \left(\frac{R_2 + \frac{j}{\omega C_2}}{R_2 + \frac{j}{\omega C_2}}\right)$$

$$Y_T = \frac{1 - j\omega C_1 \left(R_2 + \frac{j}{\omega C_2}\right)}{R_2 + \frac{j}{\omega C_2}} \cdot \left(\frac{R_2 - \frac{j}{\omega C_2}}{R_2 - \frac{j}{\omega C_2}}\right)$$

$$Y_T = \frac{R_2 - \frac{j}{\omega C_2} - j\omega C_1 \left(R_2^2 + \frac{1}{\omega^2 C_2^2}\right)}{R_2^2 + \frac{1}{\omega^2 C^2}}$$

$$Y_T = \frac{R_2 \omega^2 C_2^2 - j\omega C_2 - j\omega^3 C_1 C_2^2 R_2^2 - j\omega C_1}{1 + R_2^2 \omega^2 C_2^2}$$

$$Y_T = \frac{\omega^2 C_2 \tau - j\omega C_2 - j\omega^3 C_1 \tau^2 - j\omega C_1}{1 + \omega^2 \tau^2}$$

$$Y_T = \frac{-j\omega \left(C_1 + C_2 + C_1 \omega^2 \tau^2\right) + C_2 \omega^2 \tau}{1 + \omega^2 \tau^2}$$

Separate out the imaginary component.

$$Y_1 = -j\omega C = \frac{-j\omega \left(C_1 + C_2 + C_1 \omega^2 \tau^2\right)}{1 + \omega^2 \tau^2}$$

$$C = \frac{C_1 \left(1 + \omega^2 \tau^2\right)}{\left(1 + \omega^2 \tau^2\right)} + \frac{C_2}{1 + \omega^2 \tau^2}$$

$$C = C_1 + \frac{C_0 T_0}{T \left(1 + \omega^2 \tau^2\right)} \qquad (26\text{-a})$$

Next isolate the real component.

$$Y_2 = G = \frac{C_2 \omega^2 \tau}{1 + \omega^2 \tau^2}$$

$$G/\omega = \frac{C_0 T_0 \omega \tau}{T\ (1 + \omega^2 \tau^2)} \qquad (26\text{-b})$$

26-a and b are of precisely the same form as 19-a and b (the Debye equations). The relaxation time also has the same form. Use of this circuit analogy is the basis for the operation of the capacitance bridge, described in Appendix III.

APPENDIX III

THE CAPACITANCE BRIDGE

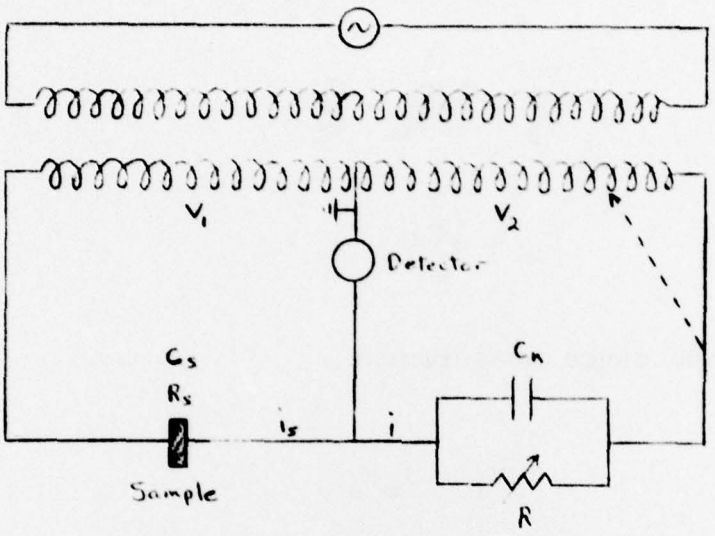

The capacitance bridge works on the principle that the dielectric sample is electrically equivalent to the circuit in Appendix II. V_1 and C_k are known constants. V_2 and R are known variables. For the capacitance measurement:

$$V_1 = \frac{i_s}{\omega C_s}$$

$$V_2 = \frac{i}{\omega C_k}$$

V_2 is adjusted until $i_s = i$, at which point no current flows through the detector. When balanced in this manner,

$$\frac{V_1}{V_2} = \frac{1/C_s}{1/C_k} = \frac{C_k}{C_s}$$

$$C_s = \frac{V_2}{V_1} C_k \quad .$$

For the conductance measurement,

$$V_1 = i_s R_s$$

$$V_2 = iR$$

When balanced ($i_s = i$),

$$R_s = \frac{V_1}{V_2} R$$

G is simply the reciprocal of R_s.

APPENDIX IV

THERMAL EXPANSION CORRECTION

Let A designate the area of a capacitor plate and x the capacitor width or any length parameter.

$$\frac{dc}{C} = \frac{dA}{A} + \frac{d\varepsilon'}{\varepsilon'} - \frac{dx}{x}$$

The x term is negative since an expansion of the thickness decreases the capacitance. Since area is proportional to length squared, the fractional change in area from thermal expansion is twice the fractional change in length. Using x as a general length variable,

$$A = \pi x^2$$

$$\frac{dA}{A} = 2\,\frac{dx}{x} \quad .$$

Therefore,

$$\frac{dc}{C} = 2\,\frac{dx}{x} + \frac{d\varepsilon'}{\varepsilon'} - \frac{dx}{x} = \frac{dx}{x} + \frac{d\varepsilon'}{\varepsilon'}$$

$$\int_{T_0}^{T} \frac{dc}{C} = \int_{T_0}^{T} \frac{dx}{x} + \int_{T_0}^{T} \frac{d\varepsilon'}{\varepsilon'}$$

$$\ell n \frac{C_T}{C_0} = \ell n \frac{\varepsilon'_T}{\varepsilon'_0} + \int_{T_0}^{T} \frac{1}{x} \frac{dx}{dT} \, dT$$

$$\ell n \frac{C_T}{C_0} = \ell n \frac{\varepsilon'_T}{\varepsilon'_0} + \int_{T_0}^{T} \alpha_p \, dT$$

$$\ell n \frac{C_T}{C_0} \frac{\varepsilon'_0}{\varepsilon'_T} = \int_{T_0}^{T} \alpha_p \, dT$$

$$\frac{C_T}{C_0} \frac{\varepsilon'_0}{\varepsilon'_T} = e^{\int_{T_0}^{T} \alpha p \, dT}$$

$$\frac{\varepsilon'_T}{\varepsilon'_0} = \frac{C_T}{C_0} e^{-\int_{T_0}^{T} \alpha_p \, dT}$$

T_0 for this study was 300°K.

UNCLASSIFIED

SECURITY CLASSIFICATION OF THIS PAGE (When Data Entered)

REPORT DOCUMENTATION PAGE

READ INSTRUCTIONS BEFORE COMPLETING FORM

1. REPORT NUMBER: U.S.N.A. - TSPR; no. 93 (1978)
2. GOVT ACCESSION NO.
3. RECIPIENT'S CATALOG NUMBER

4. TITLE (and Subtitle): (6) RADIATION INDUCED DIELECTRIC RELAXATION IN RARE-EARTH DOPED CALCIUM FLUORIDE.
5. TYPE OF REPORT & PERIOD COVERED: Final, 1977/78.
6. PERFORMING ORG. REPORT NUMBER

7. AUTHOR(s): (10) Greg C. Kolodziejczak
8. CONTRACT OR GRANT NUMBER(s)

9. PERFORMING ORGANIZATION NAME AND ADDRESS: United States Naval Academy, Annapolis, Md.
10. PROGRAM ELEMENT, PROJECT, TASK AREA & WORK UNIT NUMBERS

11. CONTROLLING OFFICE NAME AND ADDRESS: United States Naval Academy, Annapolis, Md.
12. (11) REPORT DATE: 25 May 1978
13. NUMBER OF PAGES: 64 p.

14. MONITORING AGENCY NAME & ADDRESS (if different from Controlling Office): (14) USNA-TSPR-93
15. SECURITY CLASS. (of this report): UNCLASSIFIED
15a. DECLASSIFICATION/DOWNGRADING SCHEDULE

16. DISTRIBUTION STATEMENT (of this Report)

(9) Final rept. 1977-1978.

This document has been approved for public release: its distribution is UNLIMITED.

17. DISTRIBUTION STATEMENT (of the abstract entered in Block 20, if different from Report)

This document has been approved for public release; its distribution is UNLIMITED.

(12) 68 p.

18. SUPPLEMENTARY NOTES

Accepted by the chairman of the Trident Scholar Committee.

19. KEY WORDS (Continue on reverse side if necessary and identify by block number)

Dielectric relaxation.
Rare earth fluorides.
Calcium fluorides.

20. ABSTRACT (Continue on reverse side if necessary and identify by block number)

Low frequency dielectric properties of rare-earth doped calcium fluoride crystals were studied over a temperature range of 5.5° K to 380° K.

Low flux neutron radiation was found to have no effect. - Gammarays, on the other hand, were found to significantly effect these properties. Experiment, in details, is discussed in the paper.

The results support the hypothesis that R_1 is from isolated dipoles, R_2 is from simple clusters, and R_3, R_4 and R_5 are from more complex clusters.

OVER

DD FORM 1 JAN 73 1473 EDITION OF 1 NOV 65 IS OBSOLETE
S/N 0102-LF-014-6601

UNCLASSIFIED.
SECURITY CLASSIFICATION OF THIS PAGE (When Data Entered)

245 600

The possible use of dielectrics in dosimetry also is discussed.